Polarization reversal due to charge injection in ferroelectric films

S. Bühlmann, E. Colla, and P. Muralt
Ceramics Laboratory, Engineering School, Swiss Federal Institute of Technology EPFL, CH-1015 Lausanne, Switzerland
(Received 1 December 2004; revised manuscript received 11 August 2005; published 22 December 2005)

The origin of a recently reported peculiar phenomenon—polarization reversal against the applied electric field in ferroelectric thin films [M. Aplanalp and P. Günter, Ferroelectrics **258**, 3 (2001), T. Morita and Y. Cho, Appl. Phys. Lett. **84**, 257 (2004)]—has been identified. The phenomenon is observed when poling a ferroelectric film with a large electric field applied to a conductive tip of an atomic force microscope (AFM). The effect seems to be of quite general nature as it has been observed on $BaTiO_3$ [Aplanalp *et al.*, Phys. Rev. Lett. **86**, 5799 (2001)] as well as on $LiTaO_3$ films [I. Morita and Y. Cho Appl. Phys. Lett. **84**, 257 (2004)]. It was proposed that this switching is provoked by mechanical stress due to the Maxwell force between tip and bottom electrode [Aplanalp *et al.*, Phys. Rev. Lett. **86**, 5799 (2001)]. We have studied the same phenomenon in $PbZr_{0.4}Ti_{0.6}O_3$ (PZT) thin films, deposited as epitaxial film on conductive, Nb-doped $SrTiO_3$ single crystals. New experimental evidence strongly supports a different explanation. The poling process is accompanied by considerable charge injection leading to important space charges inside the ferroelectric film. These charges finally can lead, for given conditions, to a polarization reversal when the applied voltage to the conductive AFM tip is set to zero. Two analytical models are proposed to explain field inversion in the upper part of the film.

DOI: 10.1103/PhysRevB.72.214120 PACS number(s): 77.80.Fm, 77.84.Dy, 68.37.Ps

I. INTRODUCTION

Atomic force microscope-(AFM)-assisted detection of the local piezoelectric activity in ferroelectric thin films for ferroelectric memory applications (FeRAM) represents nowadays the most popular technique to map piezoelectric activity and ferroelectric domains.[1,2] In general applying an ac electric field between the bottom electrode and the AFM tip, which scans the bare upper surface of the ferroelectric material, excites the piezoelectric converse effect. Manipulations of the polarization state are generally achieved by superimposing a stronger dc field. The field, as a consequence of the particular geometry of the tip as an electrode, is not homogeneous and can reach quite high values close to the upper surface. Studies on local poling with high electric dc fields have recently disclosed a surprising reversal of the polarization into the opposite direction compared to the poling field.[3–5] The authors of Ref. 5 give an explanation based on a combined effect of electric field and stress (ferroelastoelectricity). We have observed the reversed switching at $PbZr_{0.4}Ti_{0.6}O_3$ (PZT) thin films. In contrast, we find that the switching does not occur when the high field is applied, but later, when the dc field is set to zero. This is compatible with the observations made by the authors of Ref. 4. In this article, it is shown that the effect is based on the bilinear coupling between the electric field and polarization in the free energy G. Upon switching the sign of P_3 in an electric field E_3 where P_3 is the ferroelectric polarization and E_3 is the electric field present along the direction perpendicular to the film plane caused by injected charges, the free energy changes as $\Delta G = -2P_3E_3$.

II. EXPERIMENTAL RESULTS

The experiments were carried out on epitaxial, {100}-oriented $Pb(Zr_{0.4}Ti_{0.6})O_3$ thin films deposited on conducting $SrTiO_3$(100) single crystalline substrates doped with 2 wt% of Nb. The 50 to 400 nm thick films were grown *in situ* at 600 °C by a dynamic, reactive O_2 sputtering process using single metal targets of Pb, Zr, and Ti.[6] Further details on processing are given in Ref. 7. The films grew in cubic (100)-orientation and show at room temperature a dominant *c*-axis orientation. The *a* domains are estimated to occupy a volume fraction of 15% only. A piezoelectric response loop as observed by piezoelectric-sensitive atomic force microscopy (PAFM)[8] is shown in Fig. 1 for the 400 nm thick film. The so-observed response has to be multiplied by about a factor 5 in order to match the response observed by optical interferometry (to be published). The film is poled during

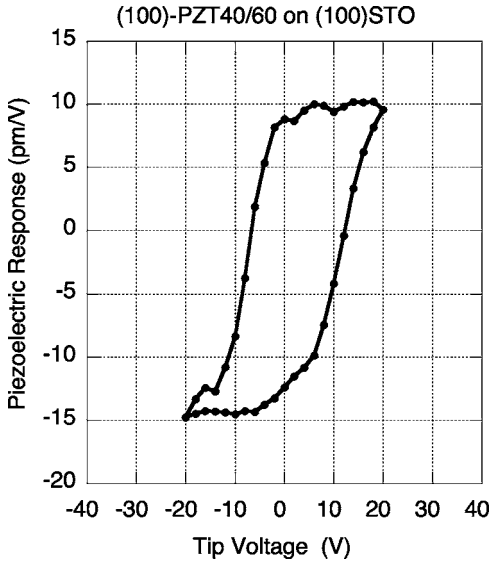

FIG. 1. Piezoelectric response loop measured by piezoelectric sensitive atomic force microscopy (PAFM).

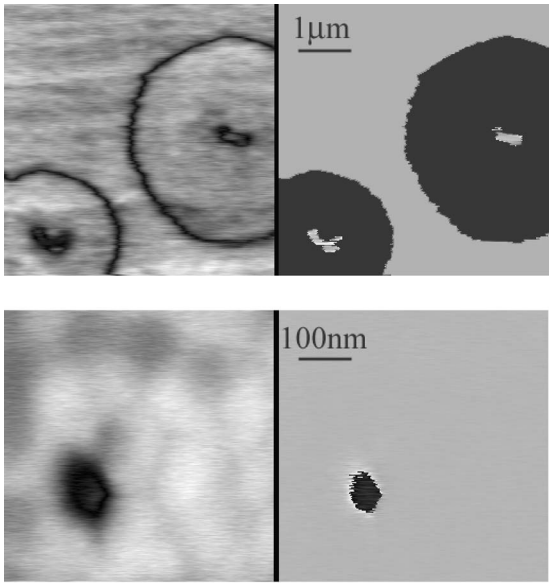

FIG. 2. Local inverse switching effects observed on 400 nm thick epitaxial PZT 40:60 $SrTiO_3$ (100) by PAFM (contact mode). (a) 5×5 μm scan after poling during 30 s at +40 V (smaller dot) and +76 V (larger dot). (b) 500×500 nm scan after poling with a 0.5 s pulse of −60 V. The as-deposited polarization is oriented upwards (bright contrast in the phase images). The images were acquired by applying 1 V (rms) at 17 kHz to the tip. The average amplitude of the tip oscillation is 6.6 pm/V.

cool down in the sputter tool. The resulting polarization points from the substrate towards the surface ("up" direction), corresponding to the polarization after application of a negative voltage to the tip. The critical switching voltages are −6.5 and +12 V for up and down switching, respectively. Note that the apparent large imprint is mostly an effect of the anisotropic electrode configuration with the tip-electrode. $d_{33,f}$ measurements with interferometry yield coercive fields of -1.10 and $+1.20\times10^7$ V/m, corresponding to switching voltages of −4.4 and +4.8 V. The tip works well as a negative electrode but is much less effective as a positive electrode.

The switching "against the electric field" was well observed on the 400 nm films. Figure 2 shows the piezoelectric response AFM (PAFM) images for both polarities of the reversed switching. The film is poled by the deposition process in the up direction, giving the bright contrast in the phase image. The images in Fig. 2(a) were taken immediately after 30 s long applications of +40 V (smaller circle) and +76 V potentials to the tip while keeping the substrate at ground. In the outer region, the polarization switched to down (dark contrast in the phase image) as expected. However, in the center where the field is highest, the polarization apparently did not switch or switched back to the previous up state. Carrying out the poling experiment with a negative voltage [Fig. 2(b)], thus applying the field parallel to the polarization, lead to an equivalent result, meaning that the polarization was switching also into the opposite direction of the applied field there where the field was highest. The polarization of the central region switched upwards; the one of the outer region did not switch. The observed reversed switching is clearly a phenomenon occurring at fields that are at least as large as three times the coercive field.

In contrast to the experiments presented in Ref. 5, the piezoelectric response was measured during the application of the large dc field. The phase of this signal clearly shows that the polarization was aligned to the electric field as long as the electric field was applied. The reversed switching thus happened after removing the large dc field. The phenomenon was not observed on the 50 nm thin film. This is compatible with Ref. 4, where it was found that a minimal thickness of 350 nm is required to observe the effect in $LiTaO_3$ films.

Suspecting this effect to be firmly related to charge injection, electrostatic force microscopy (EFM) (see Ref. 9) on poled films was carried out. This method is a useful tool to investigate charge injection in dielectrics and has also been used to investigate charge injection in polymer and nitride films (see, e.g., Ref. 10). The AFM images were collected in the noncontact mode with the cantilever vibration frequency of $f_1=70$ kHz. An ac voltage $V_0\sin(2\pi f_2 t)$ with $f_2=17$ kHz was applied between tip and substrate. The first harmonic of the cantilever response is proportional to $qV_0\sin(2\pi f_2 t)$, where q must be considered as an effective charge density per area of the film.

The film was first poled with the AFM conductive tip in contact mode, as described before. Subsequently the mode was changed to noncontact and the EFM measurements started. The EFM measurements show a strong signal due to static charges on or in the film (Fig. 3, images of rows 2, 3, and 4). Initially, the charge even shows up in the topographic image (0–12 min after stopping charge injection, images of row 2, Fig. 3) as a zone of virtual positive elevation, probably caused by strong attraction with the tip. Before injection, the phase image of the first harmonic shows a small signal with phase angle zero, as if the surface was positively charged. After injection, the response amplitude increases in a large region showing a phase of 180°, which is consistent with the existence of negative injected charges. With time, the injected charge density decays, decreasing the size of the spot.

To better elucidate the origin of the reversed polarization, the same poling procedure with an AFM was carried out on a larger scale. A film region of 4×4 μm was scanned in y mode (vertical movement of the sample) with the tip under different high voltages, from left to right. The scanning frequency was first set to 2 Hz and the number of poled points 256×256. The poling of the whole square was therefore completed within 128 s. The poling voltage was progressively increased from 20 to 90 V in order to study the direct influence of the voltage magnitude on the reversal of the polarization. An experimental detail, which will be revealed to be very important, is that just before the scanning was completed (before-last vertical line) the tip voltage was set to 0 V (short circuit with the bottom electrode) with the purpose of avoiding perturbation of the polarization state of the area during the backtrack of the tip to its rest position. The tip completed therefore the last vertical excursion on the right side of the area with 0 V, then moved back to the rest position on the left side by crossing the poled area. Subsequently the scanning mode was changed to x mode, the scanning size increased to 6×6 μm and the piezoelectric activity

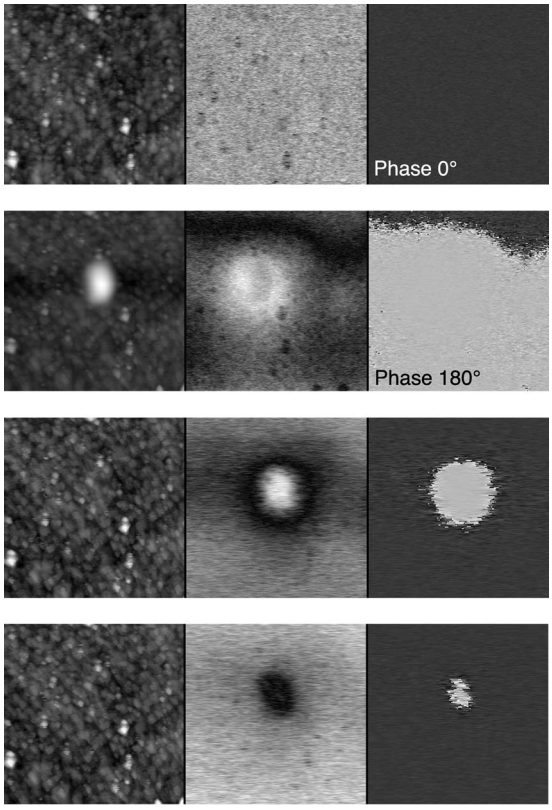

FIG. 3. 2×2 μm scans of electrostatic force microscopy (EFM) before and after poling with −80 V tip voltage during 10 s. The first scan of the poled state (second row) was started immediately after poling. The left column shows the topography, the central column the first harmonic of the amplitude, and the right column the phase of the electrostatic interaction. The experimental noncontact mode conditions (topography) were 30 nm mechanical vibration amplitude at 70 kHz. The ac electric signal was $V_{ac}=0.15V_{rms}$ at 17 kHz. Image acquisition time: 12 min.

of the whole poled region, including a surrounding frame as reference, was measured with an ac voltage of 5 Vpp (dc set to 0 V).

The expected reversed polarization could only be observed there were the tip passed over the surface of the poled sample with 0 V (Fig. 4). The reversal of the polarization did not occur during the poling at high voltage, as suspected from the small region experiments, but it was clearly provoked by the passing of the grounded tip, independently

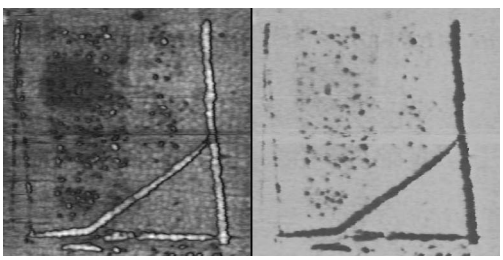

FIG. 4. 6×6 μm map of the piezoelectric response (contact mode). A 4×4 μm region in the center (roughly delimited by the frame of the reversed polarization lines) was first poled under high voltage conditions.

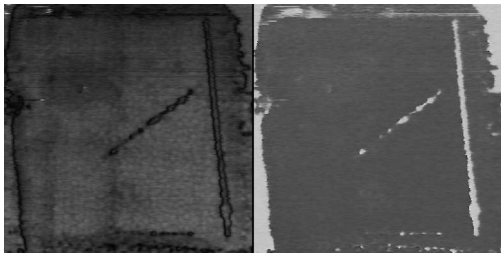

FIG. 5. Same as Fig. 3, but with opposite poling voltage and with variable scanning frequency to emphasize the time dependence of the effect.

from the magnitude of the poling voltage in the investigated range of 20-90 V. This effect is observed for both poling directions and appears to be strongly time dependent. Figure 5 was obtained by poling in the opposite direction and also with a variable scanning frequency, i.e., the first left quarter was scanned at 2 Hz, then 1 Hz, 0.5 Hz, and finally the last quarter with 0.2 Hz. Due to this variable frequency, when the tip at 0 V moved to its rest position on the left side, it crossed poled regions of very different "age." The quarter on the left was poled over 500 s before the passing of the 0 V tip, compared to about 100 s for the previous experiment. It can be seen that the reversal effect is almost absent within the first quarter.

Figure 5 shows an additional interesting feature. On the right side, the poled region exceeds by almost 1 μm the region scanned under high voltage. The sharp line with reversed polarization clearly marks the position of the tip during the last scan (at 0 V). One can therefore deduce that the application of about 80 V with a tip having a size estimated at 50 nm influences a region about 34 times larger (1.7 μm). The influence of the same tip at 0 V to reverse the polarization has a quite local effect (150–200 nm), which remains nevertheless larger than the usual resolution capabilities of writing. Figure 6 shows the same experiment on a 500 $\times$ 500 nm poled area. The movement of the tip at the end of the poling scan, after having been set at 0 V, writes the "U" with reversed polarization. When measuring regions below 200–100 nm, this effect can reverse the whole studied region, giving the impression that the reversed polarization is directly due to the high voltage.

III. DISCUSSION

The experimental findings can be summarized as follows:

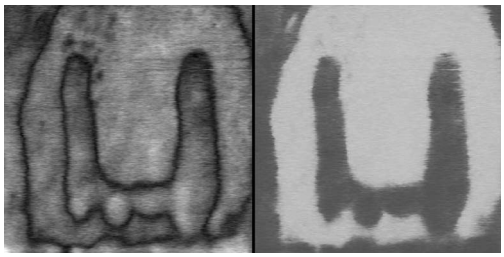

FIG. 6. 1×1 μm amplitude and phase piezoelectric activity maps. The central 500×500 nm square was poled with 80 V following the same procedure as in the previous figures.

(1) The polarization switching against the applied field requires large poling voltages (above 20 V in the 400 nm film).

(2) The switching occurs after removal of the poling voltage.

(3) The switching occurs when passing with the grounded tip in contact mode within minutes after application of the large voltage, the decay time being of the order of minutes.

(4) The reversal is observed for negative and positive poling voltage.

(5) The effect is not observed in very thin films (as, e.g., 50 nm).

These findings exclude any mechanism involving stress, as the stress is only present during application of the large voltage, i.e., when no switching occurs. In addition, the lowest order stress-polarization coupling allows only for a coupling between stress (T_3) and the square of polarization (P_3) ($T_3P_3^2$ term in free energy), which does not corroborate the stress mechanism. The reason why point (2) was not identified in Ref. 5 lays in the way they measured the piezoelectric loop. The measurement was carried out when the dc field was zero. The polarization state was changed by a voltage pulse in between the AFM measurements. Hence, their experimental results are nevertheless compatible with points (2) and (3).

To achieve a reversal of the sign, i.e., $P_3 \rightarrow -P_3$, a linear term in P_3 is needed. We propose that the electric field built up by charge injection is responsible for the polarization reversal, and that the usual bilinear term $-\mathbf{PE}$ in the free energy drives the switching to gain $\Delta G = -2P_3E_3$ in free energy density. In the following, two models are presented that can be handled by simple analytics. Exact quantitative results can only be obtained by finite element modeling. However, the basic mechanisms can be well elucidated by considering the two simple analytic models. The first model, consisting of a parallel plate capacitor, ignores the finite size of the tip radius and approximates a solution in the PZT film near the tip. It is most valid for thinner films and large tip radii. The second model, based on a totally spherical solution, includes the tip radius in the calculation. However, the finite size of the film is neglected.

First model: The ideal parallel plate capacitor defines a one-dimensional model. Indicating with the index 3 the direction perpendicular to the film plane, the electric field is obtained as $E_3 = -d\varphi/dz$ from the electric potential φ. Within the ferroelectric film of uniform polarization (no domain wall motions considered), the relevant Maxwell equation is written as follows:

$$\text{div}\, D = \frac{d}{dz}(\varepsilon_g E) = \rho,$$

$$\frac{d^2\varphi}{dz^2} = -\frac{\rho}{\varepsilon_g}. \tag{1}$$

The permittivity ε_g has been introduced to account for the polarizability of the lattice in the absence of domain wall motion and polarization switching. It is assumed that the injected charges uniformly fill the thin film. In addition, the bottom electrode at $z=0$ is kept always on ground [$\phi(0)=0$]. The tip potential at $z=h$ (film thickness h) varies according to the experimental conditions [$\phi(h)=V$]. It is further assumed that the ferroelectric charges (dP/dz) are compensated at the surface. The solution for Eq. (1) reads as

$$\varphi = -\frac{\rho}{2\varepsilon_g}(z-h)z + \frac{V}{h}z. \tag{2}$$

Charges can be injected until the field becomes zero near the top surface:

$$E_3(h) = -\varphi'(h) = \frac{\rho}{2\varepsilon_g}h - \frac{V_i}{h} = 0, \tag{3}$$

where V_i is introduced as the injection voltage. This condition defines the maximal possible charge density as follows:

$$\rho_{\max} = \frac{2\varepsilon_g V_i}{h^2}. \tag{4}$$

The PZT film used in this experiment is dominantly c-axis oriented, has a large remanent polarization (0.6 Cm^{-2}), and shows a small permittivity ε_g of 200, which practically corresponds to the one of the lattice.[11] After tip and field removal the trapped charges will stay for a while. The surface will be floating, the voltage given by charge density and the condition of zero field at the surface (no current is flowing away from the surface). When the grounded tip returns on the floating surface the condition $V=0$ in Eq. (2) must be set and it results in an electric potential due to the stored charges of

$$\varphi = -\frac{\rho}{2\varepsilon_g}(z-h)z. \tag{5}$$

The maximal possible field is derived from Eqs. (3) and (4):

$$E_{\max} = \frac{\rho_{\max}}{\varepsilon_g}(z-h/2) = \frac{2V_i}{h^2}(z-h/2). \tag{6}$$

Near the surface we obtain

$$E_{\max}(h) = \frac{\rho h}{\varepsilon_g} = \frac{V_i}{h}, \tag{7}$$

which is as large as the originally applied field $E_i = -V_i/h$, however of opposite sign! This is the field responsible for reversed switching. Since V_i was much larger than needed to switch polarization, the field of the accumulated charges will cause the switching as well. The calculated potentials are drawn in Fig. 7 and the resulting polarization configuration is shown on the right side of Fig. 8. It should be emphasized that the injected charges stabilize the tail-to-tail or head-to-head domain configurations of the polarization.

It is clear that switching proceeds faster than charge conduction. If some time elapses between injection and grounding of the surface, charges will spread out and diffuse to the bottom electrode. The time constant amounts typically to a few 100 s. Hence, after a few minutes, the charge density reaches a critical value $\rho_c = \varepsilon_g E_c/h$, below which reversed switching does not take place anymore.

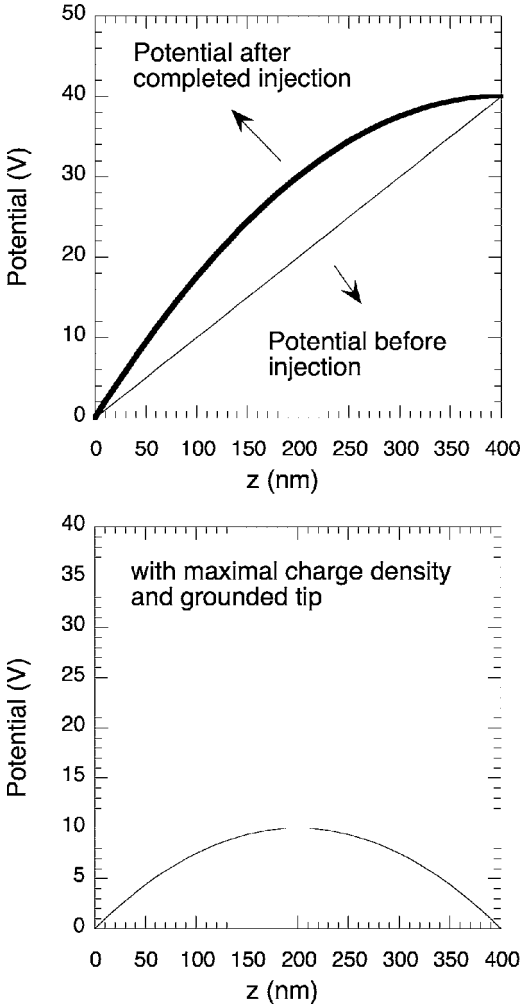

FIG. 7. Calculated electric potential for positive voltage on tip: (a) before and after saturated charge injection and (b) after grounding tip, assuming no loss of charges.

The fifth observation arises an additional question. Why does this effect work better with thicker films? Equation (7) yields an increase of $E(h)=2V_i/h$ with diminishing thickness, and thus suggests that switching should work better with thinner films. The problem of this statement is that the charge density cannot go beyond the density of potential donors and acceptors, including also deep traps. When all these sites are filled up, saturation is reached and charge injection must stop. The theory must take into account such a saturation density ρ_{sat}, which is a property of the thin film material. This density determines as well the barrier width of Schottky barriers and was thus derived from the IV characteristics of M-Fe junctions[12,13] and typically obtained as $\rho_{sat}=1.5\times10^{18}$ cm^{-3} for PZT. In thinner films, the maximal achievable electric field (E_{sat}) at the surface is thus limited by the saturation density as follows [from Eq. (6)]:

$$E_{sat}=\frac{\rho_{sat}h}{2\varepsilon_g}. \tag{8}$$

E_{sat} is an increasing function of thickness. There is thus a crossover between the two regimes. For thinner films, a critical thickness can be derived below which there is no switching:

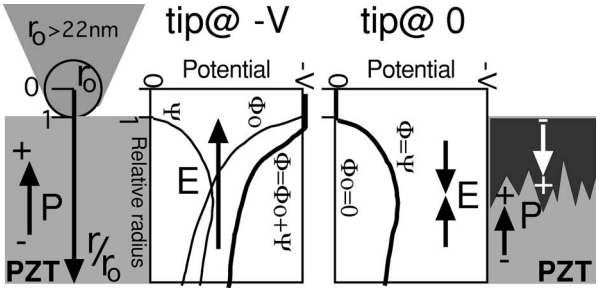

FIG. 8. Schematic presentation of the antipoling effect: (left) poling at high voltage with charge injection and (right) collection of surface charges by grounded tip and formation of opposite field in the upper part of the film, causing polarization switching. The zigzag shaped domain wall between the upper and lower film regions helps to reduce electrostatic energy of the head-to-head configuration. In the center schematic representation of the contributing potentials, according the results of the spherical model.

$$h_c=\frac{2\varepsilon_g E_c}{\rho_{sat}}. \tag{9}$$

With the (measured) coercive field of 100 kV/cm, a critical thickness of 44 nm is obtained applying $\rho_{sat}=5.0\times10^{18}$ cm^{-3}. This critical thickness comes close to experimental results, situating the threshold between 50 and 200 nm.

Second model: The second model assumes a spherical symmetry of the whole problem. A spherical tip is embedded in the ferroelectric medium. This means that the ferroelectric film thickness is much larger than the tip radius r_0. It is further assumed that the dielectric constant is the same everywhere in the ferroelectric. In this case, the electric field is a radial function and is derived as $E_r(r)=-d\varphi(r)/dr$ from the electric potential φ. The latter is linked to the charge density by means of the Poisson equation for spherical problems:

$$\Delta\varphi=\frac{d^2\varphi}{dr^2}+\frac{2}{r}\frac{d\varphi}{dr}=-\frac{\rho}{\varepsilon_g}. \tag{10}$$

The potential can be split into two parts: $\varphi(r)=V_t\varphi_0(r)+B\psi(r)$. The first function describes the situation before charge injection when the voltage V_t is applied to the tip, i.e., the situation for a dielectric free of uncompensated, trapped charges:

$$\Delta\varphi_0(r)=0, \quad \varphi_0(r)=\frac{r_0}{r}. \tag{11}$$

The initial field at the tip amounts thus to $\varphi_{init}(r_0)=V_t/r_0$. The second term accounts for the potential of the injected charges. This function ψ must be zero at $r=r_0$, decreases to zero for $r\to\infty$, never changes the sign, and such that the total potential never exceeds the value of V_t: $|\varphi(r)|\leq|V_t|$ for all values of r. A convenient function for this purpose is

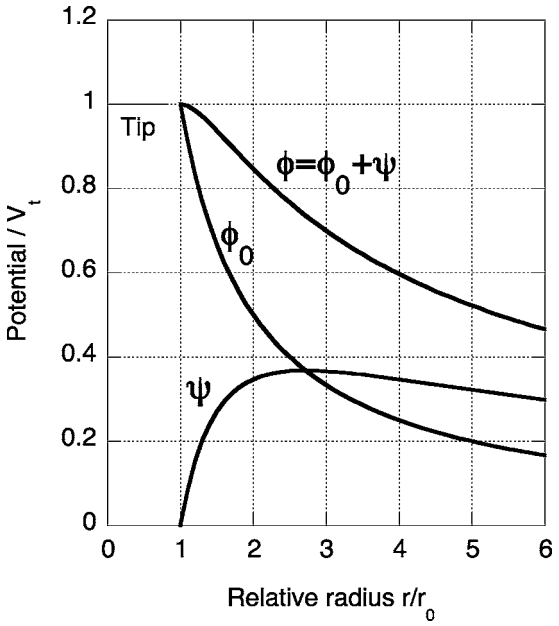

FIG. 9. Potentials versus relative radius variable. ϕ_0: initial potential before charge injection, ψ: maximal potential at which injection stops, and ϕ: total potential.

$$\psi(r) = \frac{r_0}{r} \ln\left(\frac{r}{r_0}\right). \tag{12}$$

The charge density function follows as

$$\rho(r) = \varepsilon_g B \frac{r_0}{r^3}. \tag{13}$$

The injection process stops when the field at the tip-ferroelectric interface becomes zero. This means that $B = V_t$. The maximal charge density ascribed to this situation is

$$\rho(r) = \varepsilon_g V_t \frac{r_0}{r^3}.$$

After reaching this maximum charge density, the potential becomes stationary and assumes the equilibrium potential φ_{eq} of the form

$$\varphi_{eq} = V_t\left[\frac{r_0}{r} + \frac{r_0}{r} \ln\left(\frac{r}{r_0}\right)\right]. \tag{14}$$

Its maximum is at $r = r_0$, where its derivation is zero by construction (see Fig. 9). After tip and field removal, the trapped charges will stay for a while. The surface will be floating, the voltage given by charge density and the condition of zero field at the surface (no current is flowing away from the surface). When the tip is grounded and returns on the floating surface, a potential φ_{gt} is established with $\varphi_{gt}(r_0) = 0$. The first term of the potential is vanishing. The remaining term fulfills the Poisson equation as required for $\varphi(r_0) = 0$:

$$\varphi_{gt} = V_t \frac{r_0}{r} \ln\left(\frac{r}{r_0}\right). \tag{15}$$

The electric field at the tip becomes

$$E_{gt}(r_0) = -\frac{d\varphi_{gt}}{dr} = -V_t\left[-\frac{r_0}{r^2} \ln\left(\frac{r}{r_0}\right) + \frac{r_0}{r^2}\right]_{r=r_0} = -V_t/r_0. \tag{16}$$

This field is again as large as the originally applied field, but with opposite sign, and thus is able to switch polarization near the tip. The calculated potentials are drawn in Fig. 9. The maximal potential is built up at $r_{\max} = e r_0$. The model holds if the film thickness is larger than this value, i.e., about $2 \times e$ times the tip radius at least. The tip radius in our case was specified as 30 nm. The minimal thickness thus is around 160 nm. The consequences of charge saturation by a limited defect density must be considered in this model, too. However, the solution is more delicate, because the charge density is not assumed to be constant. The highest charge density occurs just near the surface, and the limitation of this maximum value is taken into account without considering a change of the charge density function (the charges could spread into the depth of the film). The criterion is thus formulated as follows:

$$\rho(r_0) = \varepsilon_g B_{sat} \frac{1}{r_0^2} < \rho_{sat},$$

$$E_{gt,sat}(r_0) = -\frac{B_{sat}}{r_0} = \frac{\rho_{sat} r_0}{\varepsilon_g}. \tag{17}$$

E_{sat} is an increasing function of tip radius. Reversed switching is thus more likely observed with a blunt tip than with a sharp one. From the equation

$$\frac{\rho_{sat} r_0}{\varepsilon_g} > E_c \tag{18}$$

a critical tip radius is calculated as (using the same numbers as previously)

$$r_0 > \frac{\varepsilon_g E_c}{\rho_{sat}} = 22 \times 10^{-9}\ \text{m}.$$

This limit is very compatible with the applied tip having a nominal tip radius of 35 nm. The radial model thus means that we need a tip with a tip radius of more than 22 nm and a film thicker than about 120 nm (to apply the model) to observe reversed switching. This is again nicely compatible with facts. If we admit that the shape of the charge distribution changes because charges diffuse to deeper depths, the total accumulated charges would increase and smaller critical values for tip radius and film thickness would be expected.

IV. SUMMARY AND CONCLUSIONS

The polarization reversal against the applied electric field observed in ferroelectric thin films was experimentally thoroughly studied and modeled. It was disclosed that the poling

process must be accompanied by considerable charge injection leading to important space charges inside the ferroelectric film. When the tip is grounded and placed again on the poled surface, an electric field arises in the upper part of the film between the tip and the injected charges. This field is of opposite polarity as compared to the poling field. A parallel plate model and a spherical model were developed to explain the principle mechanisms responsible for this effect. In the case where the space charge is only limited by the applied voltage, both models yield the result that shortly after poling this reversed field due to space charges is as large as the poling field, and thus provokes the reversal of polarization. If the space charge density is limited by the saturation of traps in the PZT film, the two models yield a critical thickness and a critical tip radius, respectively, below which the reversed switching cannot take place, as the reversed field does not reach the coercive field limit. The known trap (acceptor, donor) densities lead to critical values of around 50 nm for the thickness and 20 nm for the tip radius. Both values are compatible with the findings of our work and the one of others. In return, reversed switching could be used to estimate such saturation trap densities. The presented strong results underline the importance of charge injection phenomena in ferroelectric films. These phenomena are expected to also occur at fields lower than those considered here and have been proposed as a key factor in fatigue mechanisms.[14]

In conclusion, the origin of the surprisingly apparent switching of the polarization against the applied electric field could be identified and the main mechanisms explained.

ACKNOWLEDGMENTS

This project was supported by the COST programs 523 and 528 and by the Swiss National Science Foundation (NCCR—Nanoscience program).

[1] A. Gruverman, H. Tokumoto, A. S. Prakash, S. Aggarwal, B. Yang, M. Wuttig, R. Ramesh, O. Auciello, and T. Venkatesan, Appl. Phys. Lett. **71**, 3492 (1997).

[2] E. L. Colla, S. Hong, D. V. Taylor, A. K. Tagantsev, and N. Setter, Appl. Phys. Lett. **72**, 2763 (1998).

[3] M. Aplanalp and P. Günter, Ferroelectrics **258**, 3 (2001).

[4] T. Morita and Y. Cho, Appl. Phys. Lett. **84**, 257 (2004).

[5] M. Aplanalp, J. Fousek, and P. Günter, Phys. Rev. Lett. **86**, 5799 (2001).

[6] S. Hiboux, P. Muralt, and T. Maeder, J. Mater. Res. **14**(11), 4307 (1999).

[7] S. Bühlmann, B. Dwir, J. Baborowski, and P. Muralt, Appl. Phys. Lett. **80**, 3195 (2002).

[8] S. Hong, J. Woo, H. Shin, J. U. Jeon, E. Y. Pak, E. L. Colla, N. Setter, E. Kim, and K. No, J. Appl. Phys. **89**, 1377 (2001).

[9] B. D. Terris, J. E. Stern, D. Rugar, and H. J. Mamin, Phys. Rev. Lett. **63**, 2669 (1989).

[10] G. C. Stevens, "Electrostatic force microscopy of charges in solid dielectrics," in *Space Charge in Solid Dielectrics*, edited by J. C. Fothergill and L. A. Dissado (The Dielectric Society, Leicester, 1998), pp. 73–92.

[11] S. Bühlmann and P. Muralt (unpublished).

[12] C. J. Brennan, Integr. Ferroelectr. **2**, 73 (1992).

[13] A. K. Tagantsev, C. Pawlaczyk, K. Brooks, and N. Setter, Integr. Ferroelectr. **4**, 1 (1994).

[14] A. K. Tagantsev, I. Stolichnov, E. Colla, and N. Setter, J. Appl. Phys. **90**, 1387 (2001).